ACS APPLIED MATERIALS & INTERFACES

Research Article

Cite This: ACS Appl. Mater. Interfaces 2019, 11, 43920−43927

www.acsami.org

Bio-orthogonal Supramolecular Latching inside Live Animals and Its Application for in Vivo Cancer Imaging

Meng Li,[†] Sungwan Kim,[‖] Ara Lee,[‡] Annadka Shrinidhi,[†] Young Ho Ko,[†] Hae Gyun Lim,[§] Hyung Ham Kim,[§] Ki Beom Bae,[⊥] Kyeng Min Park,*[,†] and Kimoon Kim*[,†,‖]

[†]Center for Self-Assembly and Complexity (CSC), Institute for Basic Science (IBS), Pohang 37673, Gyeongbuk, Republic of Korea

[‡]Division of Advanced Materials Science, [§]Department of Creative IT Engineering, and [‖]Department of Chemistry, Pohang University of Science and Technology (POSTECH), Pohang 37673, Gyeongbuk, Republic of Korea

[⊥]Advanced Bio Convergence Center, Pohang Technopark Foundation, Pohang 37668, Gyeongbuk, Republic of Korea

Supporting Information

ABSTRACT: Here, we demonstrate a supramolecular latching tool for bio-orthogonal noncovalent anchoring of small synthetic molecules in live animal models using a fully synthetic high-affinity binding pair between cucurbit[7]uril (CB[7]) and adamantylammonium (AdA). This supramolecular latching system is small (∼1 kDa), ensuring efficient uptake into cells, tissues, and whole organisms. It is also chemically robust and resistant to enzymatic degradation and analogous to well-characterized biological systems in terms of noncovalent binding. Occurrence of fluorescence resonance energy transfer (FRET) between cyanine 3-CB[7] (Cy3-CB[7]) and boron-dipyrromethene 630/650X-AdA (BDP630/650-AdA) inside a live worm (*Caenorhabditis elegans*) indicates efficient in situ high-affinity association between AdA and CB[7] inside live animals. In addition, selective visualization of a cancer site of a live mouse upon supramolecular latching of cyanine 5-AdA (Cy5-AdA) on prelocalized CB[7]-conjugating antibody on the cancer site demonstrates the potential of this synthetic system for in vivo cancer imaging. These findings provide a fresh insight into the development of new chemical biology tools and medical therapeutic systems.

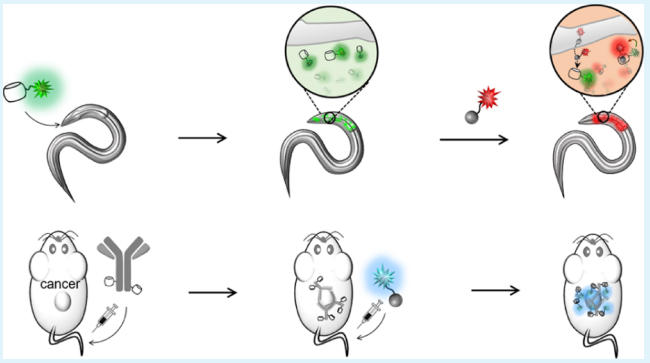

KEYWORDS: *bioimaging, host−guest chemistry, molecular recognition, cucurbituril, synthetic binding pair*

INTRODUCTION

In regions of pathogenic bacterial and viral infections in animals, selective recognition of antigens on bacteria and viruses by antibodies triggers opsonization of bacteria by macrophages and neutralization of viruses by blocking active sites.[1,2] Such important in situ biological processes occur specifically and selectively at infected sites in animals based on accurate and reliable in situ molecular recognition between biomolecules in complex and dynamic biological environments. This molecular recognition feature has been exploited as a protein-based noncovalent tool to anchor a functionality to the other materials, providing new functional materials and tools for bioapplications including targeted drug delivery and imaging.[3−7] However, typical protein-based systems are large (>100 kDa), thus requiring long treatment durations to achieve sufficient interaction with their binding partners in living organisms or fixation of tissues after taking biopsies.[8−10] Additionally, enzymatic degradation and difficulty in chemical modifications limit their uses for broad applications.[11] Synthetic binding pair systems can be alternatives for noncovalent anchoring because they are typically small (∼1 kDa), chemically tractable and scalable, and resistant to enzymatic degradation. Host−guest chemistry with macrocyclic molecules including calixarenes,[12,13] cucurbiturils,[14,15] cyclodextrins,[16−20] and pillararenes[21,22] has been extensively studied, not only to better understand recognition at the molecular level but also to develop new materials and tools.[23] Cyclodextrins and their guests, representing the most well-studied macrocyclic systems, have great potential as noncovalent binding pairs in aqueous media, as demonstrated by host−guest complexes between α-cyclodextrin and polyethyleneglycol and between β-cyclodextrin and adamantane/ferrocene (ßCD-Ad and ßCD-Fc). These binding pairs have mostly been used as pre-associated forms not dissociated by forming rotaxanes or that slowly dissociate after being applied to biological systems such as cells and animals.[16−18] Affinity-based in situ binding of cyclodextrins to their guests has been demonstrated only under simple conditions such as pure water;[19,20] in situ binding under complex and dynamic biological conditions has not yet been achieved because of a

Received: September 9, 2019
Accepted: November 5, 2019
Published: November 5, 2019

DOI: 10.1021/acsami.9b16283
ACS Appl. Mater. Interfaces 2019, 11, 43920−43927

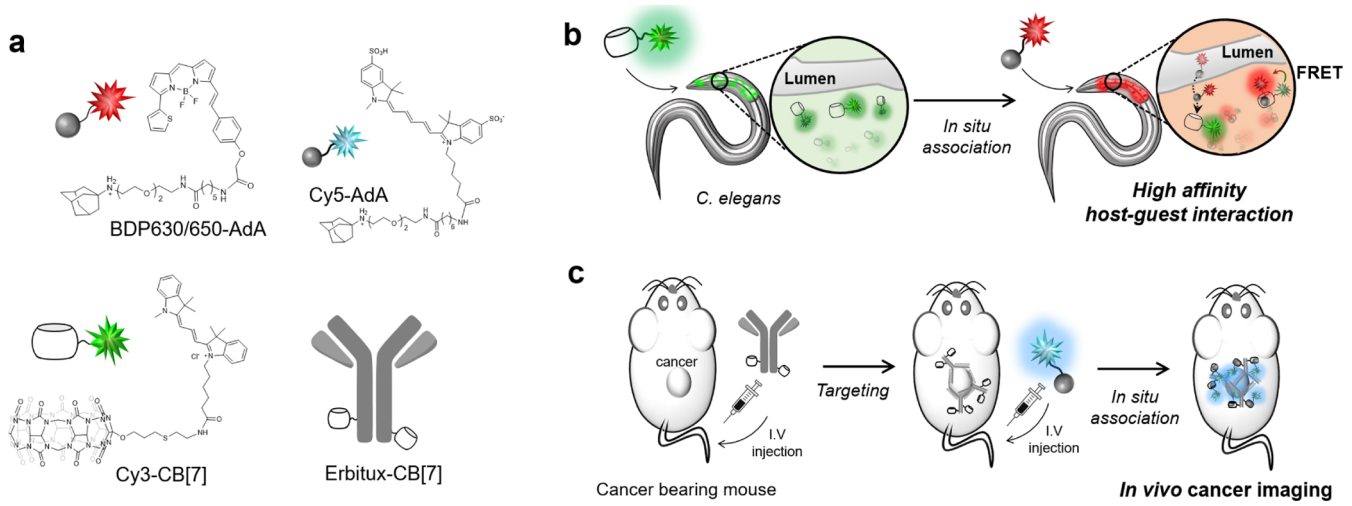

Figure 1. (a) Chemical structures of Cy3-CB[7], antibody-CB[7] (Erbitux-CB[7]), BDP630/650-AdA, and Cy5-AdA, (b) schematic illustration of locations of high-affinity host–guest interaction in live *C. elegans*, and (c) in vivo cancer imaging using the high-affinity host–guest interaction between Erbitux-CB[7] and AdA-Cy5 that are sequentially injected to a cancer-bearing mouse through the tail vein.

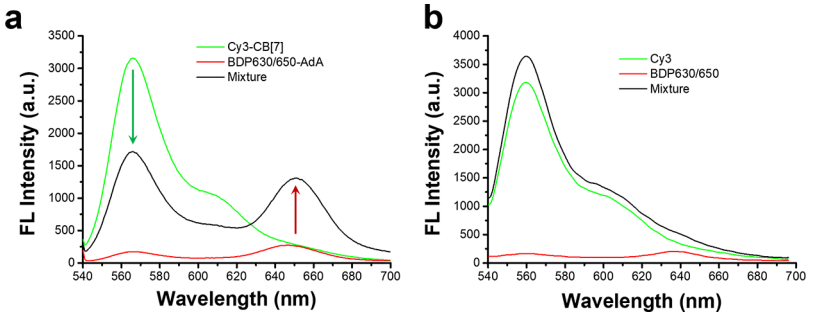

Figure 2. (a) Fluorescence emission spectra of Cy3-CB[7] only, BDP630/650-AdA only, and a mixture of Cy3-CB[7] and BDP630/650-AdA in PBS buffer containing 3% BSA. (Cy3-CB[7]) = [BDP630/650-AdA] = 500 nM. (b) Fluorescence emission spectra of Cy3 only, BDP630/650 only, and a mixture of Cy3 and BDP630/650 in PBS buffer containing 3% BSA. [Cy3] = [BDP630/650] = 500 nM (excitation at 530 nm).

significant reduction in binding fidelity through interference by other small molecules such as salts and proteins.

Recently, synthetic binding pairs with extremely high binding affinities have emerged based on cucurbit[7]uril (CB[7]), a member of a group of synthetic pumpkin-shaped macrocyclic molecules known as cucurbit[*n*]urils (*n* = 5–8, 10, 13–15) comprising *n* glycouril units with a hydrophobic cavity accessible through two identical carbonyl portals.[24−27] For example, CB[7] forms host–guest complexes with its selected guests, including ferrocenemethyl (FcA), adamantyl (AdA), and diadamantinyl ammonium derivatives, with extremely high affinity ($K_a \approx 10^{13}$ to 10^{17} M^{-1})[28] comparable to or higher than that of protein-based high-affinity binding pairs found in nature such as streptavidin–biotin ($K_a \approx 10^{13}$ M^{-1}) and antibody–antigen ($K_a \approx 10^{8}$ to 10^{13} M^{-1}).[29] Interestingly, this high-affinity molecular recognition between CB[7] and its guests takes place selectively and specifically in situ under physiological conditions and is not interfered with significantly by other biological systems, as confirmed by the occurrence of a fluorescence resonance energy transfer (FRET) signal between Cy3-CB[7][30,31] and cyanine 5-conjugated AdA (Cy5-AdA) as the donor and acceptor, respectively, inside live cells.[31] In addition, the CB[7]-based high-affinity bonds were exploited for protein imaging in cells[30] and tissues[32] and to enhance the local concentration of prodrug-conjugated adamantane (or ferrocene) in a cancer-bearing mouse.[33] These results motivated us to investigate high-affinity in situ host–guest binding in live animals using clear FRET imaging and explore the potential application of the former for active pretargeted in vivo cancer imaging.

Herein, we demonstrate supramolecular latching for tightly controlled noncovalent anchoring of a small molecule inside a simple animal model, *Caenorhabditis elegans* (*C. elegans*), using FRET between cyanine 3-conjugated-CB[7] (Cy3-CB[7]) and boron-dipyrromethene 630/650X-conjugated AdA (BDP630/650-AdA). Furthermore, we show the promising potential of this supramolecular latching system for in vivo cancer imaging by in situ bio-orthogonal anchoring of Cy5-AdA to antibody-conjugated CB[7] (Erbitux-CB[7]) pretargeted on a cancer site in a live mouse model (Figure 1).

RESULTS AND DISCUSSION

A soil nematode, *C. elegans*, as a simple animal model was used in this study before investigating with higher animals such as mice because it can be safely used in the laboratory and is inexpensive to cultivate compared with other animals such as zebrafish and mice. Furthermore, the responses of this organism to chemicals can be easily visualized by fluorescence microscopy because of their small size (~1 mm in length) and transparent body.[34] To visualize in situ high-affinity binding in worms using confocal laser scanning microscopy (CLSM), we developed a new high-affinity supramolecular FRET pair

DOI: 10.1021/acsami.9b16283
ACS Appl. Mater. Interfaces 2019, 11, 43920−43927

consisting of Cy3-CB[7] and BDP630/650-AdA as the donor and acceptor, respectively (Figure 1). Cy3-CB[7] was synthesized as described in a previous report.[30,31] BDP630/650-AdA was newly synthesized by coupling *N*-hydroxysuccinimide (NHS)-activated BDP630/650 with an adamantane amine derivative (AdA; see Experimental Section for the synthesis). We mixed Cy3-CB[7] with BDP630/650-AdA in phosphate-buffered saline (PBS) containing 3% bovine serum albumin (BSA) to mimic the crowded intracellular environment.[35] Upon excitation at 530 nm, the reduced fluorescence intensity of Cy3-CB[7] (46% at 565 nm) and the enhanced signal from BDP630/650-AdA (78% at 650 nm) clearly indicated FRET between the Cy3-CB[7] donor and BDP630/650-AdA acceptor (Figure 2a, see Experimental Section for the FRET efficiency). In a control experiment performed with free dyes (Cy3 and BDP630/650) under the same conditions, we did not observe a fluorescence change (Figure 2b), confirming that FRET occurred through the selective molecular recognition between CB[7] and AdA in a medium containing proteins.

Using this high-affinity host–guest FRET pair, we first investigated the innate fate of each FRET component (Cy3-CB[7] and BDP630/650-AdA) in live *C. elegans*. Worms were dosed with each molecule via digestive tract absorption, and we observed strong fluorescence signals for BDP630/650-AdA in intestinal cells (Figure 3b) of worms incubated with BDP630/650-AdA for 6 h before destaining for 12 h (see the Supporting Information for details). Colocalization analysis showed good overlap of fluorescence signals from BDP630/650-AdA and BODIPY 493/503 (Figure S5a), known to stain lipid droplets in intestinal cells in *C. elegans*.[36]

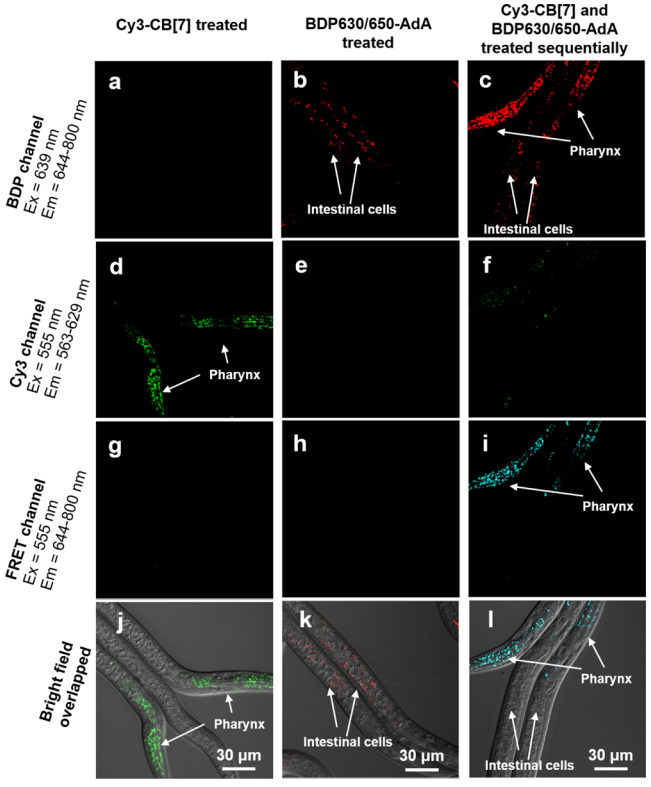

Figure 3. CLSM images of *C. elegans* incubated with (a,d,g) Cy3-CB[7] alone, (b,e,h) BDP630/650-AdA alone, and (c,f,i) Cy3-CB[7] and BDP630/650-AdA, sequentially. (j–l) Bright field images overlapped with (d,b,i), respectively. The focal plane for imaging was in the middle of worms (with the focus at the midplane, $Z = 9$ μm).

In worms treated with Cy3-CB[7], only the pharynx was stained after 12 h of incubation (Figure 3d). In a parallel experiment with a different dye-conjugated CB[7], namely, rhodamine X-conjugated CB[7] (ROX-CB[7]),[37] we also observed selective localization of ROX-CB[7] in the pharynx of worms (Figure S5c, see the Supporting Information). When worms were treated with Cy3-CB[7] whose portal was blocked with 1-adamantaneamine, a substantially reduced fluorescence signal in the pharynx was observed (Figure S7). These results indicate the importance of the CB[7] moiety of dye-CB[7]s (Cy3-CB[7] and ROX-CB[7]) for localization in *C. elegans*. In another control experiment with free Cy3 and ROX instead of Cy3-CB[7] and ROX-CB[7], respectively, free dyes did not stain cells in the pharynx; rather, the former stained cells in the intestine, and the latter did not stain any cells (Figure S6, see the Supporting Information). These observations further support a critical role for the CB[7] moiety in selective staining of the pharynx by dye-CB[7]s. Importantly, dyes for selective staining of the pharynx in *C. elegans* are not yet commercially available. Thus, we used a transgenic *C. elegans* strain (MIR8) expressing a green fluorescence protein (GFP) fusion in the pharynx and body wall muscle[38] to determine the location of dyes by colocalization analysis. Both Cy3-CB[7] and ROX-CB[7] signals overlapped well with GFP in the pharynx (Figure S5b,c, see the Supporting Information), suggesting that both dye-CB[7]s followed the same fate in live *C. elegans* (i.e., localization in the pharynx).

Next, we investigated molecular recognition between CB[7] and AdA in live *C. elegans* by sequential treatment with Cy3-CB[7] and BDP630/650-AdA for 12 and 6 h, respectively. To visualize FRET between Cy3-CB[7] and BDP630/650-AdA by CLSM, emission signals from Cy3-CB[7] and BDP630/650-AdA were collected through two different band path filters of 563–629 and 644–800 nm, respectively, upon irradiation with the same excitation laser (555 nm for Cy3 excitation). Worms treated with both sequentially displayed strong FRET signals (Figure 3i), with a significantly reduced fluorescence intensity for Cy3-CB[7] (Figure 3f) compared with worms treated only with Cy3-CB[7] (Figure 3d), indicating molecular recognition in live *C. elegans*. It is worth noting that FRET signals were strong in the pharynx of worms in which Cy3-CB[7] had already accumulated. After irradiating at the excitation wavelength of BDP630/650 (639 nm), we observed BDP630/650-AdA signals (Figure 3c) not only in the intestine but also in the pharynx, which did not show accumulation of BDP630/650-AdA when treated with BDP630/650-AdA alone (Figure 3b). These results indicate that BDP630/650-AdA recognized the prelocalized Cy3-CB[7] binding partner in the pharynx of live worms. In other words, the localization for BDP630/650-AdA was noncovalently anchored to prelocalized Cy3-CB[7] in the pharynx through high binding affinity-based in situ molecular recognition, similarly to natural protein-based binding pairs such as antigen–antibody complexes.

To validate the pivotal role of chemical moieties between CB[7] and AdA for the noncovalent anchoring in worms, we performed a control experiment with Cy3-CB[7] and free BDP630/650 without the AdA moiety following the same procedures described above. The results revealed no FRET signal and no change in the accumulation location of BDP630/650 (Figure 4). Taken together, these results demonstrate the

DOI: 10.1021/acsami.9b16283
ACS Appl. Mater. Interfaces 2019, 11, 43920–43927

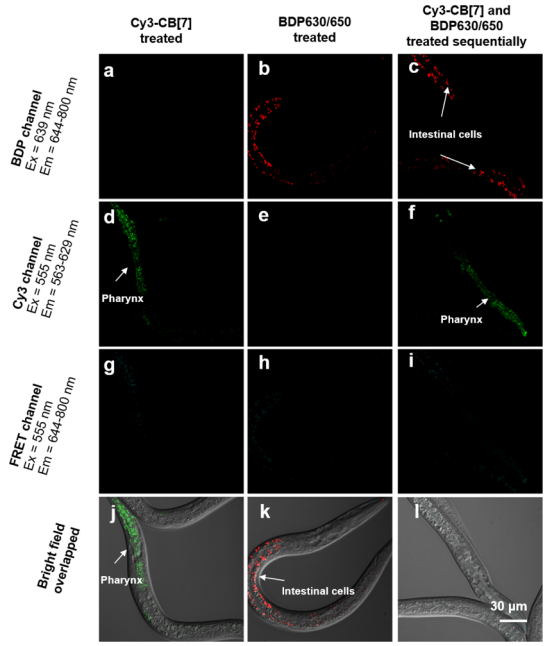

Figure 4. CLSM images of *C. elegans* incubated sequentially with (a,d,g) Cy3-CB[7] alone, (b,e,h) BDP630/650 alone, and (c,f,i) Cy3-CB[7] and BDP630/650, sequentially. (j–l) Bright field images overlapped with (d,b,i), respectively. The focal plane for imaging was in the middle of worms.

highly specific host–guest recognition between CB[7] and AdA in vivo through spontaneous FRET from Cy3-CB[7] to BDP630/650-AdA. Furthermore, it indicates supramolecular latching of BDP630/650-AdA small guest molecule on the pretreated Cy3-CB[7] host molecule in a live animal.

To confirm the above conclusion, we performed additional *C. elegans* imaging under different treatment conditions using the same FRET pair (Cy3-CB[7] and BDP630/650-AdA). Motivated by gene transfection and drug delivery across cell membranes following ultrasound stimulation that induces temporal destabilization of cell membranes by microbubble destruction (known as sonoporation)[39−42] and the endurance of *C. elegans* under ultrasound stimulation conditions,[43] we assumed that localization of Cy3-CB[7] would be altered by ultrasound stimulation, which could in turn affect the localization of BDP630/650-AdA by high-affinity-based supramolecular latching, as described above.

To validate this hypothesis, we first examined the localization of Cy3-CB[7] following a pulsed ultrasound treatment for 5 s (0.5 s per pulse) using a probe-type sonicator on live *C. elegans* during incubation with Cy3-CB[7] (see Experimental Section for details, Figures S9 and S10). It should be noted that the ultrasound treatment that we performed in this study did not appear to cause severe damage to the worms because we did not detect any differences in movement or activity from non-ultrasound-stimulated worms under an optical microscope. CLSM revealed strong fluorescence signals for Cy3-CB[7] not only in the pharynx but also under the cuticle layer when the focal plane was in the middle (midplane, $Z = 9$ μm) of live worms (Figure S8a, see the Supporting Information). By adjusting the focal plane to the ventral side (ventral midline plane, $Z = 4$ μm), allowing focused visualization on the *C. elegans* epithelial system (skin) composed of an epidermis (hypodermis) and an overlying cuticle,[44] we observed a larger number of fluorescent dots distributed throughout the entire epithelial system (Figure S8b, see the Supporting Information). These patterns and locations of the fluorescence signals from Cy3-CB[7] were distinctly different from those of non-ultrasound-stimulated worms that exhibited fluorescence signals only in the pharynx (Figures 3 and 4d). These results strongly suggest that ultrasound stimulation altered the localization of Cy3-CB[7] in live *C. elegans*.

Interestingly, Cy3-CB[7] seemed to diffuse into the epidermis across the cuticle layer during ultrasound stimulation as a result of ultrasound stimulation to *C. elegans* under four different Cy3-CB[7] incubation and washing conditions (Figure S9, see the Supporting Information for details); only when Cy3-CB[7] was located outside worms (conditions 1 and 4 in Figure S9, see the Supporting Information), Cy3-CB[7] was localized in the epithelial system of worms. This suggests that Cy3-CB[7] was confined to the pharynx and epidermis following digestive tract absorption and ultrasound stimulation, respectively. Ultrasound stimulation caused temporal destabilization of the cuticle layer, which appeared to assist the diffusion of Cy3-CB[7] across the cuticle barrier from outside.

In the case of BDP630/650-AdA, worms treated with BDP630/650-AdA alone after ultrasound stimulation and subsequently incubated for 6 h (Table S2) displayed BDP630/650-AdA fluorescence in intestinal cells (Figure 5b), similar to those without ultrasound prestimulation (Figure 3b). This indicates that the ultrasound stimulation had an

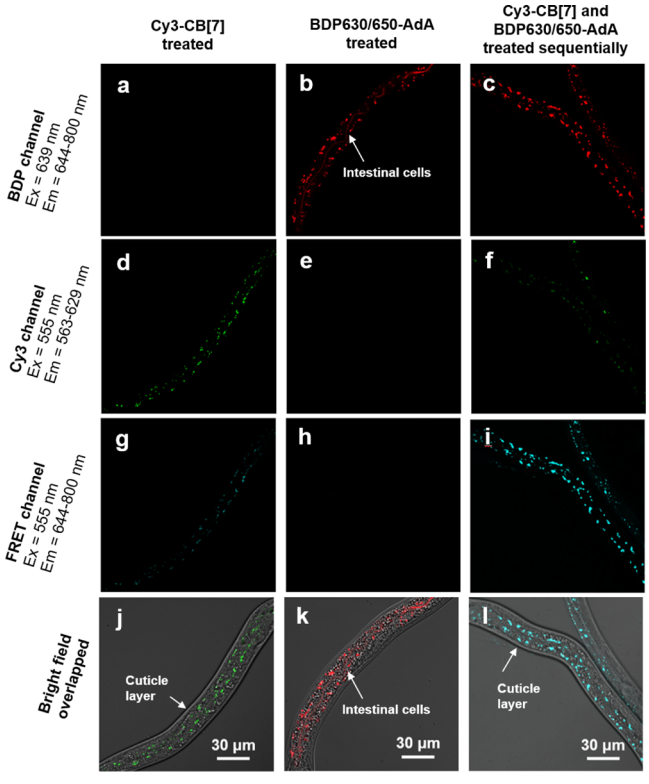

Figure 5. CLSM images of *C. elegans* (a,d,g) treated with ultrasound after Cy3-CB[7] incubation, (b,e,h) incubated with BDP630/650-AdA after ultrasound treatment, and (c,f,i) treated as in (a,d,g) but also with BDP630/650-AdA. (j–l) Bright field images overlapped with (d,b,i), respectively. Focal planes for imaging were at the ventral side (ventral midline plane, $Z = 4$ μm) and middle (midplane, $Z = 9$ μm) of the worms for (a,c,d,f,g,i) and (b,e,h), respectively (see the Suppporting Information for details).

DOI: 10.1021/acsami.9b16283
ACS Appl. Mater. Interfaces 2019, 11, 43920−43927

insignificant effect on the fate of BDP630/650-AdA in live *C. elegans*.

Next, we investigated the effect of supramolecular latching of BDP630/650-AdA on altering the localization of Cy3-CB[7] in live *C. elegans* using the FRET, as described above without ultrasound stimulation. Consistent with the results shown in Figure 3, BDP630/650-AdA still forms an in situ host–guest complex with Cy3-CB[7]; there was a strong FRET signal at the ventral midline plane near the epithelial system (Figure 5i). Given that BDP630/650-AdA was localized in intestinal cells when worms were treated with this alone (Figure 5b), the localization of BDP630/650-AdA near the epithelial system in ultrasound-stimulated worms further demonstrates noncovalent anchoring, supramolecular latching, of BDP630/650-AdA (a small molecule) on prelocalized Cy3-CB[7] via specific and stable in situ molecular recognition occurring in a complicated live animal system.

Next, we extended this supramolecular latching tool to higher animals such as mice to investigate its potential for in vivo cancer imaging. For active localization of CB[7] units on a cancer site in a mouse, the monocarboxylic acid-HEG (hexaethylene glycol)-CB[7] derivative was conjugated to Erbitux which is the trade name of cetuximab, a recombinant chimeric monoclonal antibody that targets the human epidermal growth factor receptor with high affinity for the treatment of colorectal, neck, and lung cancers.[45] Matrix-assisted laser desorption/ionization time of flight mass spectroscopy (MALDI-ToF MS) revealed successful conjugation of ca. five CB[7] units on Erbitux (Erbitux-CB[7]; Figure S11). Prior to in vivo assessments, in vitro cell experiments were performed to examine targeting ability of Erbitux after CB[7] conjugation. Almost identical fluorescence signals for the secondary antibody conjugated to Alexa 555 between both groups of cancer cells treated with Erbitux-CB[7] and Erbitux detected by CLSM (Figure 6b,c) and flow cytometry (Figure 6j) support that Erbitux retains its cancer cell targeting ability after the conjugation. Supramolecular latching of Cy5-AdA[31] to Erbitux-CB[7] on the cancer cells analyzed by CLSM (Figure 6f) and flow cytometry (Figure 6k) additionally

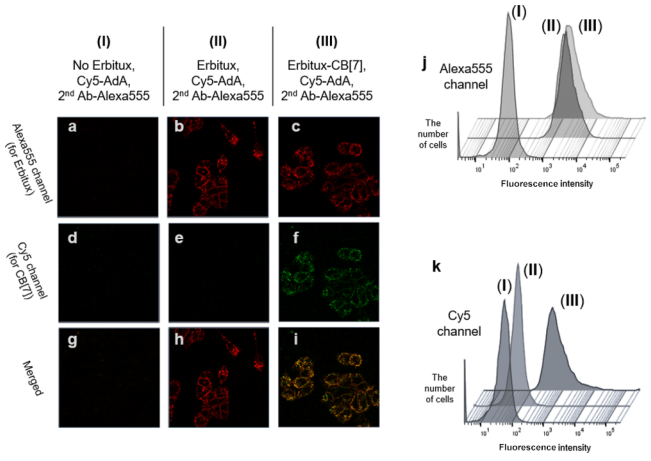

Figure 6. (a–i) CLSM images of A549 cells: (I) no primary antibody treated, but Cy5-AdA and second antibody-Alexa 555 treated, (II) Erbitux, Cy5-AdA and second antibody-Alexa 555 treated, and (III) Erbitux-CB[7], Cy5-AdA and second antibody-Alexa 555 treated, and flow cytometry results of the cells under the conditions of I, II, and III in the (j) Alexa 555 and (k) Cy5 channel.

supports not only conjugation of CB[7] units on Erbitux again but also accessibility of the cavity of CB[7] units on Erbitux to AdA using the ultrastable and bio-orthogonal host–guest chemistry. In in vivo assessments with cancer-bearing mice, only the mouse pretreated with Erbitux-CB[7] showed selective accumulation of the Cy5-AdA on the cancer site after intravenous injection of Cy5-AdA (Figure 7d). It clearly

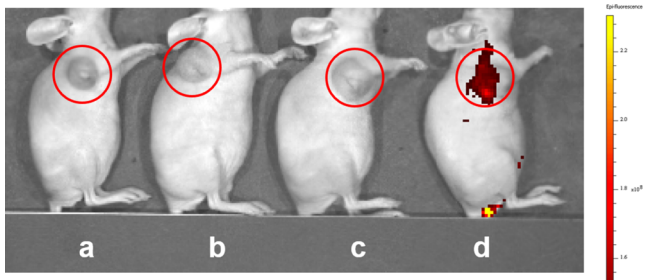

	a	b	c	d
	Non treated	Cy5-AdA	1. Erbitux 2. Cy5-AdA	1. Erbitux-CB[7] 2. Cy5-AdA
Fluorescence intensity	3.6×10^8	4.1×10^8	4.4×10^8	19.2×10^8

Figure 7. In vivo fluorescence imaging of cancer-bearing mice (a) untreated, (b) Cy5-AdA treated, (c) Erbitux and Cy5-AdA treated sequentially, and (d) Erbitux-CB[7] and Cy5-AdA treated sequentially.

demonstrates that Cy5-AdA can be noncovalently anchored on Erbitux-CB[7] that is prelocalized in a cancer site in a live mouse. This result was also cross-checked by detecting distinguishably strong fluorescence signals of Cy5-AdA from the extracted cancer tissues of the mouse treated with Erbitux-CB[7] (Figure S12d). Taken together, this noncovalent in situ anchoring, supramolecular latching, occurs efficiently under a dynamic bloodstream condition, resulting in in vivo cancer imaging of a mammalian model.

CONCLUSIONS

We have demonstrated a new supramolecular tool for noncovalent in situ anchoring of small synthetic molecules in live *C. elegans* using a fully synthetic high-affinity binding pair consisting of Cy3-CB[7] and BDP630/650-AdA. Emergence of FRET signals upon formation of an ultrastable host–guest complex between them demonstrated specific host–guest recognition in a complex biological environment inside live animals. This synthetic system appears to behave similarly to existing biological binding pairs such as antibody–antigen and cytokine-receptor systems in terms of molecular recognition in a complex environment. In addition, this synthetic system is small (~1 kDa), chemically robust and resistant to enzymatic degradation, and bio-orthogonal in binding. Incorporating an active functionality such as antibody to the synthetic host molecule allows selective imaging of a cancer site in live mouse by efficient in situ supramolecular latching of fluorescent dye-conjugated synthetic guest molecule to prelocalized host molecules on a cancer site. It clearly demonstrates the potential of this supramolecular latching system for in vivo cancer imaging. It is an example of in vivo applications of this supramolecular latching system. Even so, the system has great potential for incorporation of a wide variety of other functionalities amenable to various biological and medical

DOI: 10.1021/acsami.9b16283
ACS Appl. Mater. Interfaces 2019, 11, 43920–43927

applications owing to its synthetic tractability for chemical conjugation with not only other dyes and proteins as demonstrated here but also carbohydrates and peptides. By introducing a radioactive isotope to the small guest, this supramolecular latching system can be exploited as a fast and efficient tool for pretargeted immuno-positron emission imaging and radionuclide therapy of cancers.[46] These findings may further provide insight into the development of new chemical biological tools and medical therapeutic systems for live animals.

EXPERIMENTAL SECTION

Synthesis of BDP630/650-AdA (Scheme S1). A solution of AdA[37] (8.5 mg) in anhydrous dimethyl sulfoxide (DMSO, 200 μL) and triethylamine (2 μL) was added to BDP630/650 X NHS ester (2.0 mg) in anhydrous DMSO (100 μL, Scheme S1, see the Supporting Information). The mixture was stirred at room temperature for 3 h. The final product (2 mg, 80%) was purified by high-performance liquid chromatography and characterized by 1D and 2D NMR (Figures S1 and S2). HR-ESI-MS (m/z): [M + H^+] calcd for [$C_{45}H_{57}BF_2N_5O_5S^+$], 828.4136; found, 828.4122.

FRET Tests in Solution. The medium used for the FRET tests was 1× PBS (Lonza, catalog #: BE17-516F, 6.7 mM PO_4, without calcium and magnesium) containing 3% BSA. The fluorescence emission spectra of BDP630/650-AdA alone, Cy3-CB[7] alone, and a mixture of both the compounds were scanned from 540 to 700 nm with the same excitation wavelength (530 nm). For both compounds, the final concentration was 500 nM. The percentage decrease of fluorescence intensity from Cy3-CB[7] (donor) at 565 nm and the percentage increase of fluorescence intensity from BDP630/650-AdA (acceptor) at 646 nm were defined as follows

$$P_D = \frac{I_D - I_{DA}}{I_D} \times 100\% \quad (1)$$

$$P_A = \frac{I_{AD} - I_A}{I_{AD}} \times 100\% \quad (2)$$

where P_D is the percentage decrease of the donor at 565 nm, and I_{DA} and I_D are the donor fluorescence intensities with and without the acceptor, respectively. P_A is the percentage increase of the acceptor at 646 nm; I_{AD} and I_A are the acceptor fluorescence intensities with and without the donor, respectively.

***C. elegans* Culture.** Two types of *C. elegans* (wild-type N2 and GFP-expressed strain MIR8) were provided by Caenorhabditis Genetics Center (CGC), University of Minnesota. Briefly, *C. elegans* was cultured on solid nematode growth medium (NGM) plates and fed with a lawn of OP50 (a uracil auxotrophic *Escherichia coli* strain which grows slowly on NGM plates) or in liquid medium (S Medium with concentrated OP50 as a food source) at room temperature. For all the experiments, eggs of *C. elegans* were isolated in advance and collected in M9 buffer and then incubated in liquid medium until the L4 stage (28 h at 22 °C).

***C. elegans* Imaging with Individual FRET Compound.** Around 100 L4 stage worms were incubated in 200 μL of Cy3-CB[7] (1 μM), ROX-CB[7] (1 μM), and BDP630/650-AdA (1 μM) solution in liquid medium. After being incubated for a certain time interval (12 h for the CB[7] derivatives and 6 h for BDP630/650-AdA) on a gentle shaker (120 rpm min^{-1}) at 22 °C, the worms were washed 3 times with M9 buffer containing 0.01% Triton X-100 and destained in liquid medium (6 h for CB[7] derivatives and 12 h for BDP630/650-AdA). The worms were collected by centrifugation (1 min at 2000 rpm min^{-1}) and then treated with anesthesia (4 mg mL^{-1} levamisole) in confocal dishes for live imaging. For the colocalization of Cy3-CB[7] and ROX-CB[7] with GFP, a transgenic strain MIR8 was used instead of N2 strain.

Colocalization of BDP630/650-AdA with Lipid Droplet Tracker. Around 100 L4 stage worms were incubated in 200 μL of BDP630/650-AdA (1 μM) solution in liquid medium. After being incubated for 6 h on a gentle shaker (120 rpm min^{-1}) at 22 °C, worms were washed 3 times with M9 buffer containing 0.01% Triton X-100 to remove the remaining compound and then treated with 2 μM lipid droplet tracker BODIPY 493/503 for 12 h followed by destaining in liquid medium for 6 h. Worms were washed and collected by centrifugation and then treated with anesthesia (4 mg mL^{-1} levamisole) in confocal dishes for live imaging.

Ultrasound-Assisted Internalization of Cy3-CB[7]. Around 100 L4 stage worms were incubated in 200 μL of Cy3-CB[7] (1 μM) solution in liquid medium. Following incubation for 12 h on a gentle shaker (120 rpm min^{-1}) at 22 °C, the worms were exposed to pulsed ultrasound stimulation by using a probe sonicator (20 W) with 20% output power for 5 s (10 shots, 0.5 s per shot). The worms were cultured for another 2 h followed by washing with M9 buffer containing 0.01% Triton X-100 3 times and destained in liquid medium for 18 h on a gentle shaker. The worms were collected by centrifugation and then treated with anesthesia (4 mg mL^{-1} levamisole) in confocal dishes for live imaging. See Figure S10 for the setup.

In Vivo Host–Guest Recognition Tests in Live *C. elegans*. L4 stage worms in liquid medium were evenly divided into four groups (Table S1). The worms without any treatment were used as a blank. The other three groups were treated as follows. (1) For worms treated with both compounds sequentially, they were incubated in 400 μL of Cy3-CB[7] (1 μM) in liquid medium for 12 h, washed with M9 buffer containing 0.01% Triton X-100 3 times, and destained in liquid medium for 6 h. Then, they were incubated in 400 μL of BDP630/650-AdA (1 μM) in M9 buffer for 6 h, washed 3 times, and destained in liquid medium for 12 h. (2) For the Cy3-CB[7]-treated group, worms were incubated in 400 μL of Cy3-CB[7] (1 μM) in liquid medium for 12 h, washed 3 times, and destained for 24 h. (3) For the BDP630/650-AdA-treated group, worms were incubated in 400 μL of liquid medium for 18 h and then in 400 μL of BDP630/650-AdA (1 μM) in liquid medium for 6 h. Then, the worms were washed 3 times and destained for 12 h. After all the above treatments, the worms were treated with anesthesia (4 mg mL^{-1} levamisole) in confocal dishes for live imaging.

Synthesis of Monocarboxylic Acid-HEG-CB[7] (Scheme S2). Monoallyloxy-functionalized CB[7] (300 mg, 246 μmol)[31] and 1-mercapto-3,6,9,12,15,18-hexaoxahenicosan-21-oic acid (SH-HEG-COOH, 152 μL, 492 μmol) were added to H_2O (3 mL) in a quartz tube. After argon purging for 10 min, the mixtures were stirred for 12 h under UV light (254 nm) and dialyzed against H_2O. After being lyophilized, the product was obtained as a brown powder (200 mg, 51%). See the Supporting Information for ^1H NMR (Figure S3) and MALDI-ToF MS (Figure S4).

Synthesis of CB[7]-Conjugated Erbitux (CB[7]-Erbitux). Monocarboxylic acid-HEG-CB[7] (72 μg, 55 nmol) was added in a solution of 1-ethyl-3-(3-dimethylaminopropyl)carbodiimide (90 μg, 550 nmol) and *N*-hydroxysulfosuccinimide (180 μg, 2 μmol) in phosphate buffer silane (350 μL) and stirred for 12 h at room temperature. To the mixture, Erbitux (100 μg, 670 pmol) was added and kept at 4 °C for 2 d. CB[7]-Erbitux was obtained by washing with PBS through centrifugal filtration (MWCO: 100 kDa). Successful conjugation was confirmed by MALDI-ToF MS (Figure S11).

Immunofluorescence Imaging Using A549 Cells. A549 cells (1×10^5) were cultured in Dulbecco's modified Eagle's medium (DMEM, Hyclone) containing 10% fetal bovine serum (FBS, Hyclone) and 1% penicillin and streptomycin, and were transferred onto each confocal dish and incubated for 24 h. Erbitux or Erbitux-CB[7] (2 μg each) in 1 mL of DMEM containing 10% FBS and 1% penicillin–streptomycin (PS) was added to the cells. After 30 min of incubation in a humidified 5% CO_2 atmosphere at 37 °C, the cells were washed with PBS and treated with Alexa 555-labeled antihuman second antibody (2 μg) in 1 mL of DMEM. After 30 min of incubation at the incubator, the cells were washed with PBS and treated with Cy5-AdA in DMEM (200 nM, 1 mL). After incubation for 30 min at the incubator, cells were washed with PBS and added in DMEM (1 mL), and fluorescence intensity of each sample was

DOI: 10.1021/acsami.9b16283
ACS Appl. Mater. Interfaces 2019, 11, 43920–43927

visualized by CLSM with excitation at 488 and 633 nm for Alexa 555 and Cy5, respectively.

Flow Cytometry. A549 cells (1×10^6) in DMEM (1 mL) containing 10% FBS and 1% PS were transferred to a centrifuge tube. Erbitux or Erbitux-CB[7] (2 μg each) in 1 mL of DMEM containing 10% FBS and 1% PS was added to the cells. After 30 min of incubation in a humidified 5% CO_2 atmosphere at 37 °C, the cells were washed with PBS (1 mL) for 3 times. Additionally, the same process was carried out with Cy5-AdA in DMEM (200 nM, 1 mL) and Alexa 555-labeled antihuman secondary antibody (2 μg) in 1 mL of DMEM, sequentially. Finally, the cells were resuspended with 200 μL of PBS and analyzed by using a flow cytometry machine with excitation at 488 and 633 nm for Alexa 555 and Cy5, respectively.

Preparing Cancer-Bearing Mice. All the animal experiments were conducted with appropriate permission from the animal rights commission of the Advanced Bio Convergence Center, Pohang Technopark Foundation. A549 cells were inoculated subcutaneously (s.c.) at a density of 1×10^7 cells per mouse into the flank of each female balb/c mouse weighing 20 g. The cancer cells inoculated were left for approximately 3 weeks until the tumors reached 5−10 mm in size.

In Vivo Imaging of Cancer on Mice. The mice were randomly divided into four groups and intravenously injected with PBS (200 μL), Erbitux (100 μg in 200 μL of PBS), or CB[7]-Erbitux (100 μg in 200 μL of PBS). After 24 h of injection, PBS (200 μL) or Cy5-AdA (200 μL, 200 nM in PBS) was injected to the mice. After 6 h of uptake, whole body imaging and ex vivo imaging were performed and analyzed with an IVIS spectrum small-animal in vivo imaging system (Caliper Life Sciences).

Biodistribution of Cy5-AdA and Region of Interest Values of Cy5-AdA from Extracted Organs. After the final imaging, mice (n = 3) were sacrificed, and major organs (tumor, muscle, spleen, liver, kidney, heart, and lung) were collected for detecting fluorescence signals of Cy5-AdA by using the IVIS machine (ex. = 640 nm, em. = 700 nm). The radiance (photon emission per unit area) of a region of interest in each organ was acquired by using ImageJ software (Figure S12).

■ ASSOCIATED CONTENT

Supporting Information

The Supporting Information is available free of charge on the ACS Publications website at DOI: 10.1021/acsami.9b16283.

Synthetic scheme and NMR spectra for BDP630/650-AdA, experimental conditions for treating *C. elegans* with FRET elements, CLSM images of *C. elegans* treated with FRET elements, illustration of a setup for ultrasound treatment, and fluorescence images of extracted organs of cancer-bearing mice (PDF)

■ AUTHOR INFORMATION

Corresponding Authors

*E-mail: kmpark@ibs.re.kr (K.M.P.).
*E-mail: kkim@postech.ac.kr (K.K.).

ORCID

Kyeng Min Park: 0000-0001-6089-6169
Kimoon Kim: 0000-0001-9418-3909

Author Contributions

M.L. and S.K. contributed equally to this work. M.L. performed synthesis and *C. elegans* experiments. S.K. performed synthesis and mice experiments and A.L. performed *C. elegans* experiments. Y.H.K. analyzed NMR experiments and A.S. performed synthesis of a dye. H.G.L. and H.H.K. supported ultrasound stimulation experiments. K.B.B. supported mice experiments. M.L., K.M.P., and K.K. wrote the manuscript. K.M.P. and K.K. supervised the work.

Notes

The authors declare no competing financial interest.

■ ACKNOWLEDGMENTS

This work was supported by the Institute for Basic Science (IBS) [IBS-R007-D1] (to K.K.) and the National Research Foundation of Korea (NRF) grant funded by the Korea government (MSIT) (No. NRF-2019R1A2C2010484) (to H.H.K). A.L. acknowledges a National Research Foundation of Korea (NRF) grant funded by the Korean government (NRF-2017H1A2A1044903-Global Ph.D. Fellowship Program).

■ REFERENCES

(1) Medzhitov, R. Recognition of Microorganisms and Activation of the Immune Response. *Nature* **2007**, *449*, 819−826.
(2) Nimmerjahn, F.; Ravetch, J. V. Fc Gamma Receptors as Regulators of Immune Responses. *Nat. Rev. Immunol.* **2008**, *8*, 34−47.
(3) Gao, X.; Cui, Y.; Levenson, R. M.; Chung, L. W. K.; Nie, S. In Vivo Cancer Targeting and Imaging with Semiconductor Quantum Dots. *Nat. Biotechnol.* **2004**, *22*, 969−976.
(4) Ruan, J.; Song, H.; Qian, Q.; Li, C.; Wang, K.; Bao, C.; Cui, D. HER2 Monoclonal Antibody Conjugated RNase-A-Associated CdTe Quantum Dots for Targeted Imaging and Therapy of Gastric Cancer. *Biomaterials* **2012**, *33*, 7093−7102.
(5) Drake, P. M.; Rabuka, D. An Emerging Playbook for Antibody-Drug Conjugates: Lessons from The Laboratory and Clinic Suggest a Strategy for Improving Efficacy and Safety. *Curr. Opin. Chem. Biol.* **2015**, *28*, 174−180.
(6) Allen, T. M. Ligand-Targeted Therapeutics in Anticancer Therapy. *Nat. Rev. Cancer* **2002**, *2*, 750−763.
(7) Scott, A. M.; Wolchok, J. D.; Old, L. J. Antibody Therapy of Cancer. *Nat. Rev. Cancer* **2012**, *12*, 278−287.
(8) Rothbauer, U.; Zolghadr, K.; Tillib, S.; Nowak, D.; Schermelleh, L.; Gahl, A.; Backmann, N.; Conrath, K.; Muyldermans, S.; Cardoso, M. C.; Leonhardt, H. Targeting and Tracing Antigens in Live Cells with Fluorescent Nanobodies. *Nat. Methods* **2006**, *3*, 887−889.
(9) Herce, H. D.; Schumacher, D.; Schneider, A. F. L.; Ludwig, A. K.; Mann, F. A.; Fillies, M.; Kasper, M.-A.; Reinke, S.; Krause, E.; Leonhardt, H.; Cardoso, M. C.; Hackenberger, C. P. R. Cell-Permeable Nanobodies for Targeted Immunolabelling and Antigen Manipulation in Living Cells. *Nat. Chem.* **2017**, *9*, 762−771.
(10) Fu, J.; Yu, C.; Li, L.; Yao, S. Q. Intracellular Delivery of Functional Proteins and Native Drugs by Cell-Penetrating Poly(disulfide)s. *J. Am. Chem. Soc.* **2015**, *137*, 12153−12160.
(11) Beck, A.; Wurch, T.; Bailly, C.; Corvaia, N. Strategies and Challenges for The Next Generation of Therapeutic Antibodies. *Nat. Rev. Immunol.* **2010**, *10*, 345−352.
(12) Mutihac, L.; Lee, J. H.; Kim, J. S.; Vicens, J. Recognition of Amino Acids by Functionalized Calixarenes. *Chem. Soc. Rev.* **2011**, *40*, 2777−2796.
(13) Qin, Z.; Guo, D.-S.; Gao, X.-N.; Liu, Y. Supra-Amphiphilic Aggregates Formed by *p*-Sulfonatocalix[4]arenes and The Anti-psychotic Drug Chlorpromazine. *Soft Matter* **2014**, *10*, 2253−2263.
(14) Park, K. M.; Murray, J.; Kim, K. Ultrastable Artificial Binding Pairs as a Supramolecular Latching System: A Next Generation Chemical Tool for Proteomics. *Acc. Chem. Res.* **2017**, *50*, 644−646.
(15) Kim, K.; Selvapalam, N.; Ko, Y. H.; Park, K. M.; Kim, D.; Kim, J. Functionalized Cucurbiturils and Their Applications. *Chem. Soc. Rev.* **2007**, *36*, 267−279.
(16) Li, J.; Li, X.; Ni, X.; Wang, X.; Li, H.; Leong, K. W. Self-Assembled Supramolecular Hydrogels Formed by Biodegradable PEO−PHB−PEO Triblock Copolymers and α-Cyclodextrin for Controlled Drug Delivery. *Biomaterials* **2006**, *27*, 4132−4140.
(17) Singh, A.; Zhan, J.; Ye, Z.; Elisseeff, J. H. Modular Multifunctional Poly(ethylene glycol) Hydrogels for Stem Cell Differentiation. *Adv. Funct. Mater.* **2013**, *23*, 575−582.

DOI: 10.1021/acsami.9b16283
ACS Appl. Mater. Interfaces 2019, 11, 43920−43927

(18) Zhang, J.; Ma, P. X. Cyclodextrin-Based Supramolecular Systems for Drug Delivery: Recent Progress and Future Perspective. *Adv. Drug Delivery Rev.* **2013**, *65*, 1215−1233.
(19) Harada, A.; Kobayashi, R.; Takashima, Y.; Hashidzume, A.; Yamaguchi, H. Macroscopic Self-Assembly Through Molecular Recognition. *Nat. Chem.* **2011**, *3*, 34−37.
(20) Yamaguchi, H.; Kobayashi, Y.; Kobayashi, R.; Takashima, Y.; Hashidzume, A.; Harada, A. Photoswitchable Gel Assembly Based on Molecular Recognition. *Nat. Commun.* **2012**, *3*, 603.
(21) Xue, M.; Yang, Y.; Chi, X.; Zhang, Z.; Huang, F. Pillararenes, A New Class of Macrocycles for Supramolecular Chemistry. *Acc. Chem. Res.* **2012**, *45*, 1294−1308.
(22) Duan, Q.; Cao, Y.; Li, Y.; Hu, X.; Xiao, T.; Lin, C.; Pan, Y.; Wang, L. pH-Responsive Supramolecular Vesicles Based on Water-Soluble Pillar[6]arene and Ferrocene Derivative for Drug Delivery. *J. Am. Chem. Soc.* **2013**, *135*, 10542−10549.
(23) Ma, X.; Zhao, Y. Biomedical Applications of Supramolecular Systems Based on Host−Guest Interactions. *Chem. Rev.* **2015**, *115*, 7794−7839.
(24) Isaacs, L. Stimuli Responsive Systems Constructed Using Cucurbit[*n*]uril-Type Molecular Containers. *Acc. Chem. Res.* **2014**, *47*, 2052−2062.
(25) Masson, E.; Ling, X.; Joseph, R.; Kyeremeh-Mensah, L.; Lu, X. Cucurbituril Chemistry: A Tale of Supramolecular Success. *RSC Adv.* **2012**, *2*, 1213−1247.
(26) Kim, K.; Murray, J.; Selvapalam, N.; Ko, Y. H.; Hwang, I. *Cucurbiturils*; World Scientific: Europe, 2018.
(27) Barrow, S. J.; Kasera, S.; Rowland, M. J.; del Barrio, J.; Scherman, O. A. Cucurbituril-Based Molecular Recognition. *Chem. Rev.* **2015**, *115*, 12320−12406.
(28) Assaf, K. I.; Nau, W. M. Cucurbiturils: from Synthesis to High-Affinity Binding and Catalysis. *Chem. Soc. Rev.* **2015**, *44*, 394−418.
(29) Shetty, D.; Khedkar, J. K.; Park, K. M.; Kim, K. Can We Beat The Biotin-Avidin Pair?: Cucurbit[7]uril-Based Ultrahigh Affinity Host-Guest Complexes And Their Applications. *Chem. Soc. Rev.* **2015**, *44*, 8747−8761.
(30) Kim, K. L.; Sung, G.; Sim, J.; Murray, J.; Li, M.; Lee, A.; Shrinidhi, A.; Park, K. M.; Kim, K. Supramolecular Latching System Based on Ultrastable Synthetic Binding Pairs as Versatile Tools for Protein Imaging. *Nat. Commun.* **2018**, *9*, 1712.
(31) Li, M.; Lee, A.; Kim, K. L.; Murray, J.; Shrinidhi, A.; Sung, G.; Park, K. M.; Kim, K. Autophagy Caught in The Act: A Supramolecular FRET Pair Based on An Ultrastable Synthetic Host-Guest Complex Visualizes Autophagosome-Lysosome Fusion. *Angew. Chem., Int. Ed.* **2018**, *57*, 2120−2125.
(32) Sasmal, R.; Das Saha, N.; Pahwa, M.; Rao, S.; Joshi, D.; Inamdar, M. S.; Sheeba, V.; Agasti, S. S. Synthetic Host−Guest Assembly in Cells and Tissues: Fast, Stable, and Selective Bioorthogonal Imaging via Molecular Recognition. *Anal. Chem.* **2018**, *90*, 11305−11314.
(33) Zou, L.; Braegelman, A. S.; Webber, M. J. Spatially Defined Drug Targeting by in Situ Host−Guest Chemistry in a Living Animal. *ACS Cent. Sci.* **2019**, *5*, 1035−1043.
(34) Hulme, S. E.; Whitesides, G. M. Chemistry and The Worm: *Caenorhabditis elegans* as A Platform for Integrating Chemical and Biological Research. *Angew. Chem., Int. Ed.* **2011**, *50*, 4774−4807.
(35) Ellis, R. J. Macromolecular Crowding: an Important but Neglected Aspect of the Intracellular Environment. *Curr. Opin. Struct. Biol.* **2001**, *11*, 114−119.
(36) Klapper, M.; Ehmke, M.; Palgunow, D.; Böhme, M.; Matthäus, C.; Bergner, G.; Dietzek, B.; Popp, J.; Döring, F. Fluorescence-Based Fixative and Vital Staining of Lipid Droplets in *Caenorhabditis elegans* Reveal Fat Stores using Microscopy and Flow Cytometry Approaches. *J. Lipid Res.* **2011**, *52*, 1281−1293.
(37) Li, M.; Lee, A.; Kim, S.; Shrinidhi, A.; Park, K. M.; Kim, K. Cucurbit[7]uril-Conjugated Dyes as Live Cell Imaging Probes: Investigation on Their Cellular Uptake and Excretion Pathways. *Org. Biomol. Chem.* **2019**, *17*, 6215−6220.
(38) Schmeisser, K.; Mansfeld, J.; Kuhlow, D.; Weimer, S.; Priebe, S.; Heiland, I.; Birringer, M.; Groth, M.; Segref, A.; Kanfi, Y.; Price, N. L.; Schmeisser, S.; Schuster, S.; Pfeiffer, A. F. H.; Guthke, R.; Platzer, M.; Hoppe, T.; Cohen, H. Y.; Zarse, K.; Sinclair, D. A.; Ristow, M. Role of Sirtuins in Lifespan Regulation is Linked to Methylation of Nicotinamide. *Nat. Chem. Biol.* **2013**, *9*, 693−700.
(39) Unga, J.; Hashida, M. Ultrasound Induced Cancer Immunotherapy. *Adv. Drug Delivery Rev.* **2014**, *72*, 144−153.
(40) Deckers, R.; Moonen, C. T. W. Ultrasound Triggered, Image Guided, Local Drug Delivery. *J. Controlled Release* **2010**, *148*, 25−33.
(41) Canavese, G.; Ancona, A.; Racca, L.; Canta, M.; Dumontel, B.; Barbaresco, F.; Limongi, T.; Cauda, V. Nanoparticle-Assisted Ultrasound: A Special Focus on Sonodynamic Therapy Against Cancer. *Chem. Eng. J.* **2018**, *340*, 155−172.
(42) Stewart, M. P.; Langer, R.; Jensen, K. F. Intracellular Delivery by Membrane Disruption: Mechanisms, Strategies, and Concepts. *Chem. Rev.* **2018**, *118*, 7409−7531.
(43) Ibsen, S.; Tong, A.; Schutt, C.; Esener, S.; Chalasani, S. H. Sonogenetics is a Non-Invasive Approach to Activating Neurons in Caenorhabditis elegans. *Nat. Commun.* **2015**, *6*, 8264.
(44) Chisholm, A. D.; Hsiao, T. I. The *Caenorhabditis elegans* Epidermis as a Model Skin. I: Development, Patterning, and Growth. *Wiley Interdiscip. Rev.: Dev. Biol.* **2012**, *1*, 861−878.
(45) Bou-Assaly, W.; Mukherji, S. Cetuximab (Erbitux). *Am. J. Neuroradiol.* **2010**, *31*, 626−627.
(46) Strebl, M. G.; Yang, J.; Isaacs, L.; Hooker, J. M. Adamantane/Cucurbituril: A Potential Pretargeted Imaging Strategy in Immuno-PET. *Mol. Imaging* **2018**, *17*, 1536012118799838.

DOI: 10.1021/acsami.9b16283
ACS Appl. Mater. Interfaces 2019, 11, 43920−43927